Impacts of Relative Sea-level Rise on Evolution of Shallow Estuaries

Carl T. Friedrichs[1], David G. Aubrey[1], and Paul E. Speer[2]

[1]Woods Hole Oceanographic Institution
Woods Hole, MA 02543

[2]Center for Naval Analyses
Alexandria, VA (temporarily at[1])

ABSTRACT

The present study investigates the impact of relative sea-level rise on tidal propagation in shallow, well-mixed estuaries. Distortion of the co-oscillating estuarine tide is a composite of two principal non-linear effects: frictional interaction between the tide and channel (reflected in the scale a/h, or ratio of tidal amplitude to mean channel depth) and intertidal storage on tidal flats and marshes (measured by Vs/Vc, or ratio of volume of intertidal storage to volume of channels at mean sea level). Estuarine hypsometry (distribution of estuary surface area with height) defines a/h and Vs/Vc, and indicates whether these parameters will increase or decrease with increasing water level. The potential impact of sea-level rise is investigated utilizing both one-dimensional numerical modeling and seasonal fluctuations in mean sea levels at six shallow estuaries along the U.S. Atlantic Coast. These fluctuations are used as analogues to interannual trends in mean sea level rise. Numerical results and analysis of tidal propagation at the selected estuaries indicate that in flood dominant estuaries having relatively constant bank slope (rectangular or trapezoidal cross-section), a/h and degree of tidal distortion decrease with increased sea level. In estuaries having highly curved bank slope, a/h and Vs/Vc increase in flood and ebb dominant systems, increasing the degree of distortion and reinforcing existing tidal asymmetries. These findings have implications for the evolution of shallow estuaries as global sea level rises (an anticipated consequence of increased atmospheric trace gas loading). Whether estuaries import or export increased amounts of sediments as global sea-level rises depends on local estuarine geometry. Some systems will infill faster as sea level rises, while some will flush more efficiently. These contrasting responses to mean sea-level rise mandate a careful assessment of how any individual estuary may respond to rising water levels.

I. Introduction

Increased atmospheric trace gas loading and resulting climate change, may cause global mean sea level to rise on the order of one to several meters over the next century (NRC 1979; Hoffman et al., 1983). The position of the shoreline will change, and to some degree, the dynamics of coastal processes will be altered (Giese and Aubrey, 1987; NRC, 1987). Among the environments to show clear effects of encroaching seas along passive and barrier-type coastlines will be tidal lagoons and estuaries. The hydrodynamics of tidal estuaries are important to navigation, fisheries, flooding, and general water quality, as well as to the geological evolution of the coastline. One can use directly observable seasonal sea-level fluctuations in tidal inlets, channels and bays to infer the initial impact of

relative sea-level rise on tidal dynamics (Aubrey and Friedrichs, 1988). In temperate zones, monthly mean sea level varies annually on the order of 30 cm due to variations in wind set-up, atmospheric pressure and water density. Continuous sea surface elevation data spanning a year or more in duration enable the examination of tidal variations under a range of oceanographic and climatological conditions analogous to the sea-level rise anticipated during coming decades.

One particularly relevant measure of estuarine hydrodynamics pertains to the distortion of the tide as it propagates through these shallow systems. Non-linear tidal distortion is a useful parameterization of tidal hydrodynamics, important to sediment transport and consequently to the evolution of shallow tidal estuaries (e.g., Postma, 1967; Boon and Byrne, 1981; Aubrey, 1986). "Flood dominant" lagoons and estuaries (having shorter duration, higher velocity floods) tend to infill their channels with coarse sediment. "Ebb dominant" systems (having shorter, higher velocity ebbs) tend to flush near-bed sediment seaward more effectively, and may represent more stable geometries (Speer and Aubrey, 1985; Aubrey, 1986). Observations taken from existing estuarine systems combined with numerical modeling results indicate that non-linear tidal distortion is primarily a result of frictional interaction with the channels and intertidal storage in tidal flats and marshes. Friction in shallow channels slows the propagation of low water through the inner estuary, shortening the duration of flood, whereas extensive intertidal storage slows the propagation of high water, shortening the duration of ebb. Strongly flood dominant systems are typically shallow (tidal amplitude/mean depth > ~0.3), having only small-to-moderate storage capacity in intertidal flats and marshes. Strongly ebb dominant estuaries are relatively deeper (a/h < ~0.25) and exhibit greater intertidal water storage (Aubrey and Speer, 1985; Friedrichs and Aubrey, 1988).

If shallow, flood dominant estuaries tend to shoal and deeper, ebb dominant channel systems tend to scour, then flood and ebb dominant systems should engender continued flood and ebb dominant behavior, respectively. Neglecting such important processes as storm overwash and transport of suspended sediment, this line of reasoning suggests that tidally dominant estuaries evolve into two geometrically and hydrodynamically divergent groups. However if present trends continue, rising global sea level has the potential of perturbing this divergence. If rising mean sea level causes channel depth to increase significantly or alters the volume of water stored intertidally, then the sense of tidal distortion and resulting sediment transport patterns may be altered fundamentally.

The distortion of a tide in bays and estuaries can be modeled as a non-linear growth of compound constituents and harmonics of the principal astronomical tidal components (e.g., Dronkers, 1964; Boon and Byrne, 1981; Uncles, 1981; Speer and Aubrey, 1985). Transfer of energy to even harmonics can produce asymmetric tidal velocities which result in net transport of coarse near-bed sediment and of suspended load. Along coastlines where the dominant astronomical constituent is M_2, the most significant overtide formed in well-mixed estuaries is M_4, the first harmonic of M_2. If estuarine tidal elevation is modeled as

$$A = a_{M2}\cos(\omega t - \theta_{M2}) + a_{M4}\cos(2\omega t - \theta_{M4}) \tag{1}$$

where t is time, ω is M_2 tidal frequency, a is amplitude and θ is phase, then the amplitude ratio and relative phase of M_4 to M_2 are defined as

$$M_4/M_2 = a_{M4}/a_{M2} \tag{2}$$

$$2M_2 - M_4 = 2\theta_{M2} - \theta_{M4} \tag{3}$$

Flood and ebb dominant systems have relative sea surface phases of 0-180 and 180-360 degrees, respectively. For a fixed relative phase, the larger the M_4/M_2 ratio, the greater the magnitude of distortion and the more strongly flood or ebb dominant the system becomes.

II. Numerical Modeling

The physics of non-linear tidal distortion are investigated with a one-dimensional numerical model (Speer and Aubrey, 1985). One-dimensional approximations assume a small horizontal aspect ratio (channel depth/width<<1), long narrow channels (width/length<<1), and a well-mixed water column. The governing equations are conservation of mass and linear momentum:

$$\frac{\partial \zeta}{\partial t} + \frac{1}{b}\frac{\partial U}{\partial x} = 0 \tag{4}$$

$$\frac{\partial U}{\partial t} + \frac{\partial}{\partial x}\frac{U^2}{A} = -g\,A\,\frac{\partial \zeta}{\partial x} - \frac{\tau_b}{\rho}\,P \tag{5}$$

where $\zeta(x,t)$ = sea surface elevation, $U(x,t)$ = volume flux, τ_b = average shear stress on channel solid boundaries, ρ = density of water, P = channel wetted perimeter, A = channel cross-sectional area, and b = width of channel and flats. Friction is formulated as:

$$\tau_b = \rho f\,\frac{|U|}{A}\,\frac{U}{A} \tag{6}$$

where f is a dimensionless friction factor. The model approximates an ideal shallow estuary having two distinct elements: (1) a trapezoidal channel that transports all the momentum of the system and (2) shallow, sloping intertidal flats that act in a storage capacity only (Figure 1a). The boundary conditions on the model are M_2 surface forcing at the ocean end and no flux at the inland end. For systems modeled in this study, principal non-linear effects enter through friction in the momentum equation and through tidal interactions with estuarine geometry in the continuity equation (Speer and Aubrey, 1985).
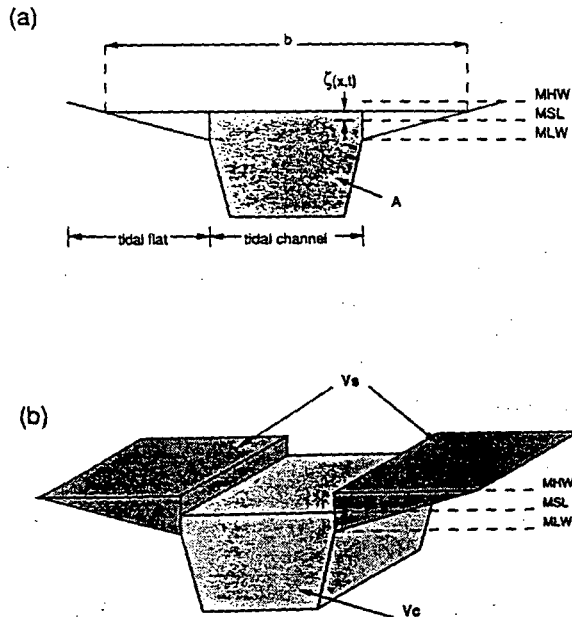
(a)

(b)

FIGURE 1. Schematic representations of the model system: (a) The numerical model is drawn in cross-section, showing the division of the model into (i) a momentum carrying channel and (ii) tidal flats which act in a storage capacity only. b = model width; $\zeta(x,t)$ = sea surface height; A = channel cross-sectional area, MHW, MSL and MLW = mean high water, mean sea level and mean low water. (b) A block diagram illustrates Vs = volume of storage in intertidal areas and Vc = mean volume in channels.

To quantify those morphological features of shallow estuaries relevant to the generation of non-linear tidal distortion, geometric parameters must be defined. The non-dimensional ratio a/h is defined as offshore M_2 amplitude divided by mean estuarine channel depth. In the shallow systems considered in this study, a/h scales the depth effect on bottom friction. A second non-dimensional ratio, Vs/Vc (Figure 1b), is defined as the volume of water stored, Vs, between mean high and low water in tidal flats and marshes divided by the volume of water contained in channels, Vc, at mean sea level (channels are defined as those areas submerged at mean low water). Vs and Vc represent the two dynamically distinct regions modeled numerically (flats which act in a storage capacity only and a momentum transporting channel). Vs/Vc scales the tidal interactions with estuarine geometry in the continuity equation (Friedrichs and Aubrey, 1988).

Numerical calculations of non-linear tidal distortion as a function of the geometric parameters (Friedrichs and Aubrey, 1988) are used to infer changes in distortion with sea-level rise. Once Vs/Vc and a/h are determined as functions of mean sea level for any given tidal estuary, probable trends in distortion can be determined. The distribution of non-linear distortion forms two fields, flood and ebb dominance, separated by the 180° contour in the $2M_2$-M_4 plot (Figure 2). This line corresponds to a trough in the contour plot of M_4/M_2. Among flood dominant systems, M_4/M_2 is primarily a function of a/h, whereas among ebb dominant systems it is primarily a function of Vs/Vc (Figure 2a). Relative phase is a more complicated function of both Vs/Vc and a/h (Figure 2b). Friedrichs and Aubrey (1988) confirmed trends in the numerical results by comparison to tide gauge records from 22 shallow tidal estuaries, and by examination of the non-linear response to variations in semi-diurnal tidal amplitude during the spring neap cycle. Numerical results represent average distortion of a symmetric ocean tide measured at four stations along a 7 km long estuary channel. The plots do not include the effects of system length or existing offshore tidal asymmetries, either of which can have a significant impact on non-linear tidal distortion (Dronkers, 1986; Friedrichs and Aubrey, 1988). However, initial increases in ocean height (tens of centimeters) will likely have a more significant impact on a/h and Vs/Vc than on channel length or distortion of the offshore tide.
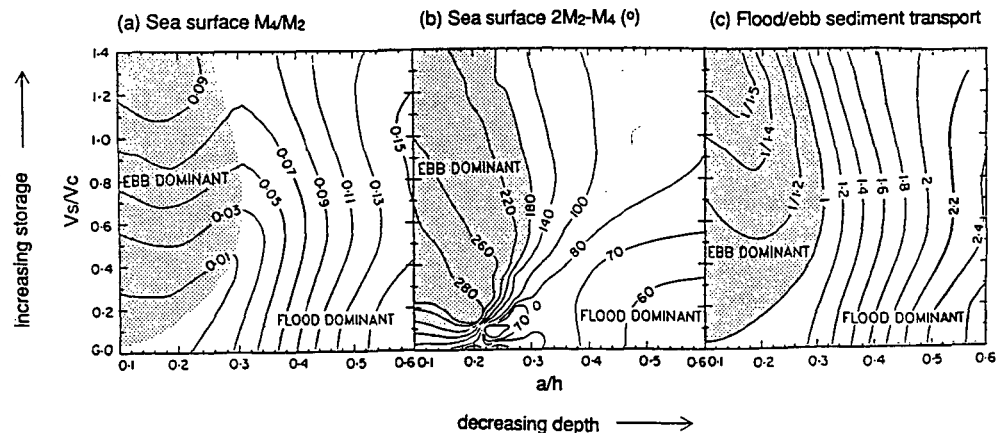

FIGURE 2. Contour plots of the parameters which determine non-linear tidal distortion as a function of a/h and Vs/Vc, resulting from 84 model systems (after Friedrichs and Aubrey, 1988): (a) surface M_4/M_2 amplitude ratio; (b) surface $2M_2$-M_4 relative phase; (c) flood-to-ebb near-bed sediment transport ratio. The distribution of non-linear distortion forms two fields, flood and ebb dominance, separated by the 180° contour in $2M_2$-M_4. Numerical results for coarse sediment transport are similar to trends in M_4/M_2 sea surface distortion.

Calculations of asymmetry in near-bed, coarse sediment transport (Figure 2c) produce trends that are similar to those in sea surface M_4/M_2 (Figure 2a). Therefore variations in sea surface distortion with sea-level rise can be used as reasonable indicators of probable changes in near-bed transport patterns (Friedrichs and Aubrey, 1988). Following Aubrey (1986) theoretical flood-to-ebb near-bed transport ratios are produced utilizing cross-sectionally averaged velocities obtained from numerical modeling and the transport formula of Meyer-Peter and Muller (1948). Results of numerical modeling suggest that changes in near-bed sediment transport with sea-level rise will be determined primarily by changes in a/h or Vs/Vc in flood or ebb dominant estuaries, respectively.
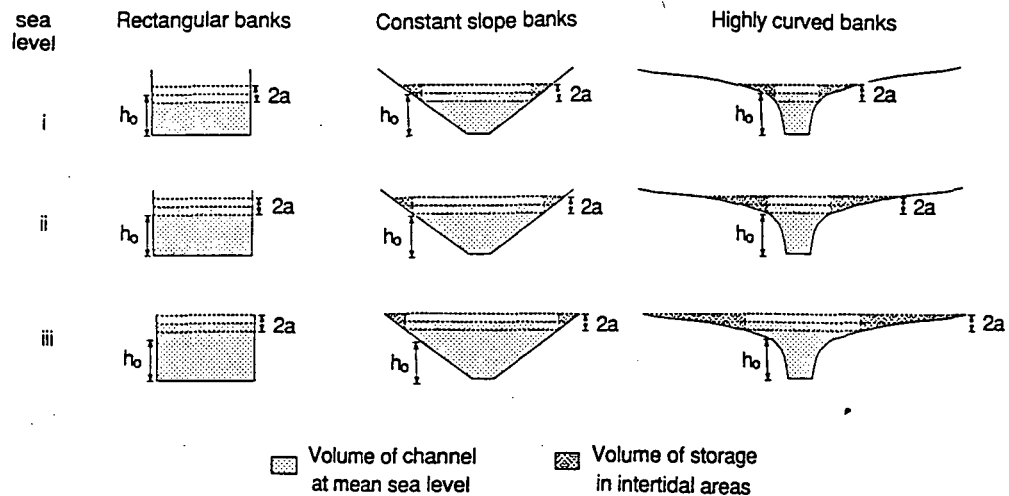

FIGURE 3. Cross-sections of conceptual rectangular, constant bank slope and highly curved bank slope channels at three sea-levels. h_o = reference depth and 2a = tidal range. Geometric parameters for each channel, measured at each of the three sea levels are displayed in Figure 4.

III. Geometry and Sea Level

To apply the numerical and empirical relationships between geometry and distortion to changes in global ocean height, the dependence of a/h and Vs/Vc on relative sea level must be determined. For a rectangular channel (Figure 3), the surface area of the system remains constant with depth. Because the channel banks are vertical, cross-sectionally averaged depth is equal to depth at the channel mid-point, and both increase by an amount equal to sea-level rise (Figure 4). Changes in geometry due to sea-level rise can be described fully by changes in a/h. If the cross-section is modeled with banks of constant slope (Figure 3), mean channel depth is less than that at the mid-point, and mean depth increases by an amount less than sea-level rise (Figure 4). In the constant slope model the Vs/Vc ratio is no longer zero. Vs remains constant with sea-level rise, so Vs/Vc decreases as Vc increases. If the cross-section of a shallow estuary has highly curved bank slopes (Figure 3), the response of a/h and Vs/Vc to sea-level rise can be markedly different. As sea level rises, shallows which were once beyond the edge of the channel are flooded and incorporated into the now wider channel. Including these newly flooded shallows into the channel can cause mean channel depth to decrease. In contrast to the rectangular and constant bank slope cases, a/h will then increase with mean sea-level rise (Figure 4). Also, if the bank slope is strongly curved, as sea level rises the areas submerged intertidally can increase dramatically, causing the Vs/Vc ratio to increase. Since the geometric parameters determine the type of distortion, changes in distortion and therefore near-bed transport with sea-level rise will be strongly dependent on bank slope.

The different bank slopes illustrated in Figures 3 and 4 provide insight into non-linear tidal response with sea-level rise at existing shallow tidal estuaries. Figure 5 shows hypsometric curves (profiles of surface area versus depth) at six tidally dominated estuaries. Bank slope can be derived directly from the hypsometric curve if the slope is averaged along the estuary. Main Creek, SC, and Little River, SC, (Figure 5a, b) exhibit only a slight decrease in bank slope with elevation, whereas Price, SC, and Wachapreague, VA, (Figure 5c, d) display highly curved bank slopes, with highest curvature occurring near the level of low tide. Manasquan, NJ, and Oaks Creek, SC, (Figure 5e, f) have more complicated geometries. The two extreme hypsometric groupings (relatively constant or highly curved bank slope) are analogous to the differences in the conceptual estuarine cross sections in Figure 3. With higher sea level, these basic differences in hypsometry cause opposite trends in non-linear tidal response.
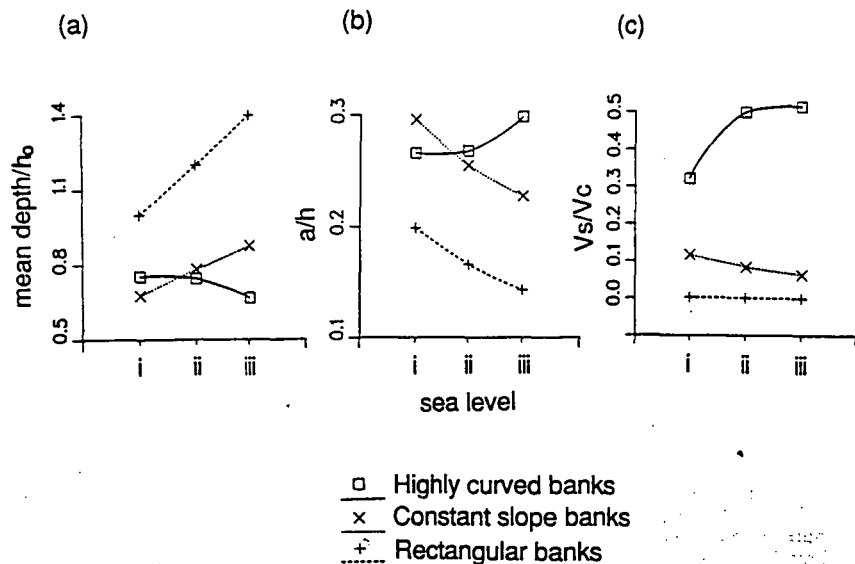

FIGURE 4. Changes in geometric parameters with sea-level rise in three conceptual model channels: effect of sea level on (a) mean channel depth, (b) a/h and (c) Vs/Vc. Response of geometric parameters to sea level is strongly dependent on system geometry.

Map views of these systems illustrate the differences in hypsometry. Main Creek and Little River (Figure 6) are shallow (average channel depth 2-2.5 m at MSL) and have marsh widths of 2 km or less measured perpendicular to the shoreline. In contrast, Price and Wachapreague (Figure 7) are significantly deeper (mean channel depths of 3.5-4 m) and have much wider marshes (5-10 km). Extensive intertidal mud flats contribute to highly curved bank slope. The surface area of flats at Price and Wachapreague is 4-5 times that of channels (FitzGerald and Nummedal, 1983; Byrne et al., 1975) but at Main Creek and Little River flats cover only 0.7 or less times the area of channels (Aubrey and Friedrichs, 1988; NOAA chart 11534). With limited marsh, narrow flats and shallow channels, the bank slopes of Main Creek and Little River are relatively constant; whereas with extensive marsh, large mud flats and deep channels, the bank slopes of Price and Wachapreague are strongly curved. Manasquan and Oaks Creek (Figure 8) contain features of each end member: they are at least as shallow as Main Creek or Little River, but they also exhibit sharp discontinuities in hypsometry near low tide, like Price and Wachapreague.

Quantitative changes in the geometric parameters with changes in sea level can be determined directly from the hypsometric curves. Mean sea level, low and high water, and the hypsometric curve define areas which can be integrated to determine a/h and Vs/Vc for any given sea level (Figure 9). Published hypsometries and
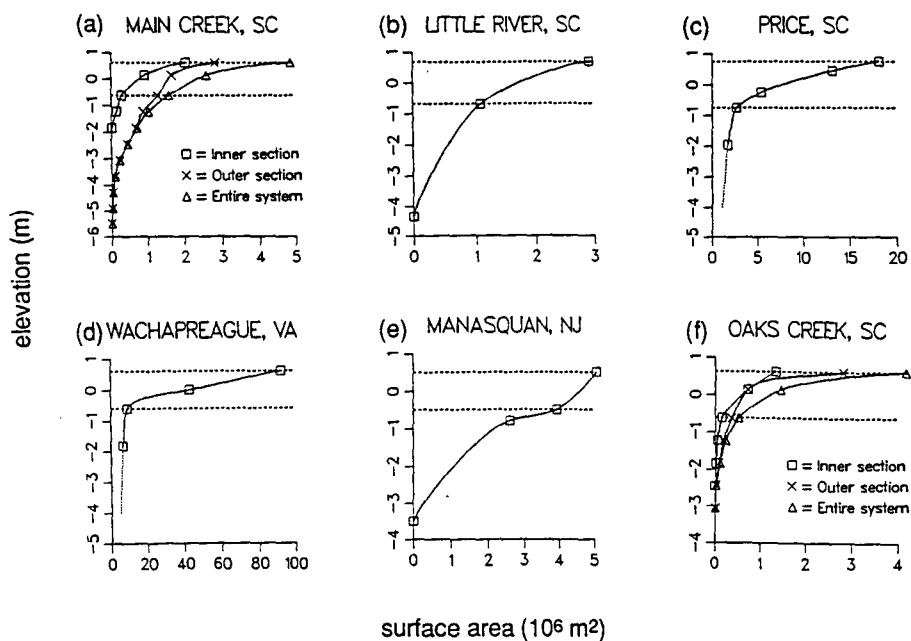
FIGURE 5. Hypsometric curves (estuarine surface area vs. elevation) for six tidally dominated estuaries: (a) Main Creek, SC; (b) Little River, SC; (c) Price, SC; (d) Wachapreague, VA; (e) Manasquan, NJ; (f) Oaks Creek, SC. Dashed lines show mean levels of high and low water within the estuaries.
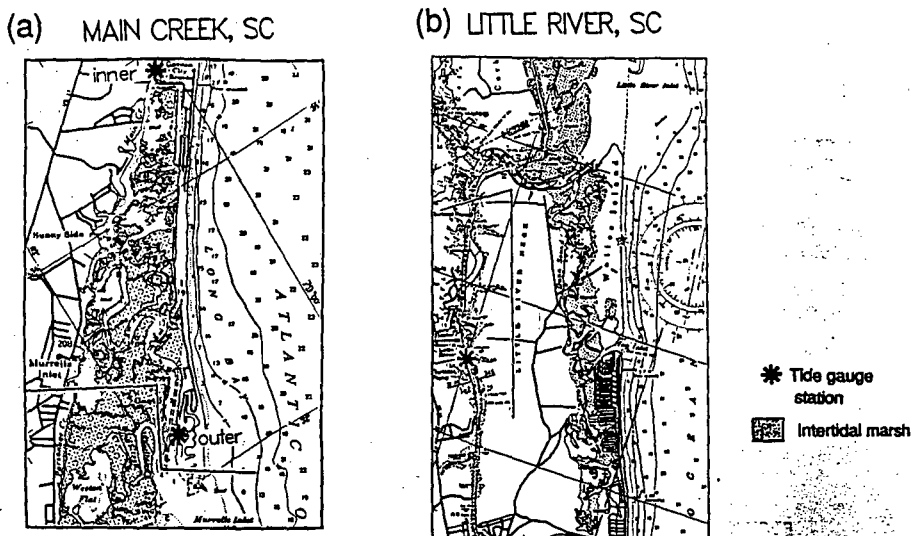

FIGURE 6. Bathymetric maps of flood dominant systems with relatively constant bank slope (after NOAA chart 11534): (a) Main Creek, SC; (b) Little River, SC. Heavy black lines crossing tidal channels and marsh indicate boundaries for purposes of geometric parameters. Soundings are depth in feet at mean low water (1 ft. = .305m). Scale is given by lines of latitude (two minutes = 3,704m).

PRICE, SC   ✳ Tide gauge
                      station
               ▦ Intertidal marsh
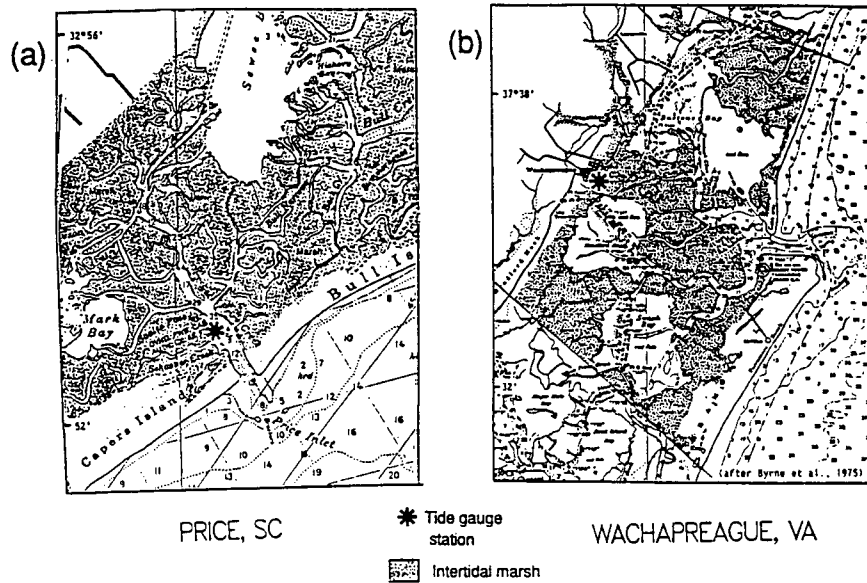
WACHAPREAGUE, VA

FIGURE 7. Bathymetric maps of ebb dominant systems with highly
curved bank slopes: (a) Price Creek, SC (after NOAA chart 11531);
(b) Wachapreague, VA (after Byrne et al., 1975). The entire
tidal drainage area for each inlet is considered in calculating
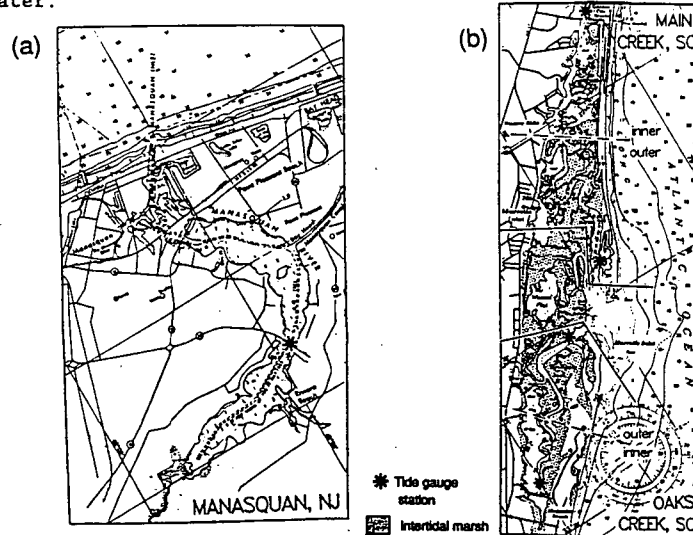geometric parameters. Soundings are depth in feet at mean low
water.

FIGURE 8. Bathymetric map of flood dominant systems with highly
curved and banked slopes: (a) Manasquan, NJ (after NOAA chart
12324); (b) Oaks Creek and neighboring Main Creek, SC (after NOAA
chart 11534). Heavy black lines crossing tidal channels and
marsh indicate boundaries for purposes of geometric parameters.
Dashed lines separate Oaks Creek and Main Creek into inner and
outer sections for analyzing local changes in distortion and
geometry. The entire tidal drainage area of the inlet is
considered in calculating geometric parameters in Manasquan.
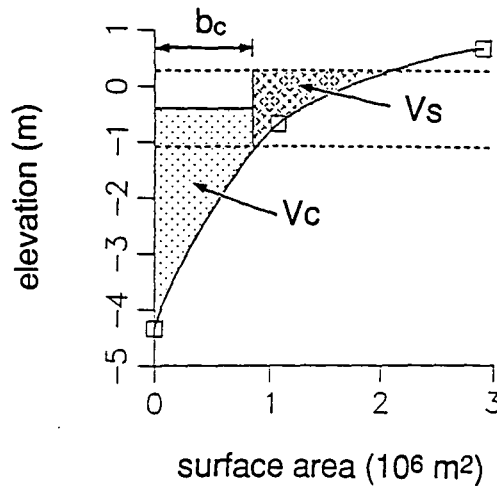Soundings are depth in feet at mean low water.

FIGURE 9. Methodology for determining geometric parameters from Little River, SC hypsometric curve. Vc (volume of channels) is the region between the hypsometric curve and low water plus the product of estuarine tidal amplitude and b_c (low water surface area). V_s is the region with surface area greater than b_c, bounded by the hypsometric curve and the high and low water lines. Mean channel depth is given by Vc divided by b_c.

topographic charts (Table 1) commonly depict the level of mean high water, but not the detailed information needed to determine bank slope for the first tens of centimeters above high water. Therefore, it is necessary to compare the geometric parameter values at present sea level with those at slightly reduced sea level to evaluate trends in Vs/Vc due to marginal changes in sea level (Table 2).

Table 1. Sources of hypsometric and sea height data used in calculation of geometric and non-linear distortion parameters:

Estuary	Geometry source	Sea surface record	Sea height source
Main Creek, SC	Perry et al., 1978	10/01/74-01/31/76	NOS 1985; Aubrey and Friedrichs 1988
Little River, SC	NOAA chart 11534	07/30/74-09/28/74 11/21/74-05/13/75	NOS 1985
Price, SC	Fitzgerald and Nummedal 1983 (low to high water) USGS topos Sewee Bay/ Capers, SC (subtidal)	09/01/75-02/18/76; 06/08/76-09/16/76; 12/01/77-12/31/77	NOS 1985
Wachapregue, VA	Byrne et al., 1975	01/01/83-12/31/83	Boon, personal communication
Manasquan, NJ	USGS topo Point Pleasant, NJ	04/12/76-06/30/77	NOS 1985
Oaks Creek, SC	Perry et al., 1978	10/01/74-01/31/76	NOS 1985; Aubrey and Friedrichs 1988

Values determined for Vs/Vc at present sea level disagree with Friedrichs and Aubrey (1988) by 30% and 65% for Wachapreague, Va. and Main Creek, S.C., respectively. This discrepancy is mainly due to measurement of Vs in the previous study using estimates of tidal prism rather than changes in surface area with height. In the case of Main Creek, Friedrichs and Aubrey determined tidal prism by the empirical equation of Jarrett (1976) relating tidal prism to inlet cross-sectional area. Disagreement between values for Vs based on marsh outlines depicted on navigation maps and those based on empirical relationships to inlet size is not unexpected. It is not clear which of these methods is more accurate in the absence of detailed field studies (with goals specifically including measurements of tidal prism or intertidal hypsometry). Friedrichs and Aubrey (1988) examined the geometries of 22 systems to overcome uncertainties in individual measurements. The potential impact of errors inherent in estimates of intertidal storage (and the other geometric parameters) can also be minimized by examining responses to spring-neap amplitudes (Boon, 1988; Friedrichs and Aubrey, 1988) or seasonal mean sea level (Aubrey and Friedrichs, 1988). Trends in tidal distortion due to spring-neap and seasonal cycles in individual systems are determined by fewer variables than the more extreme differences in distortion observed between systems.
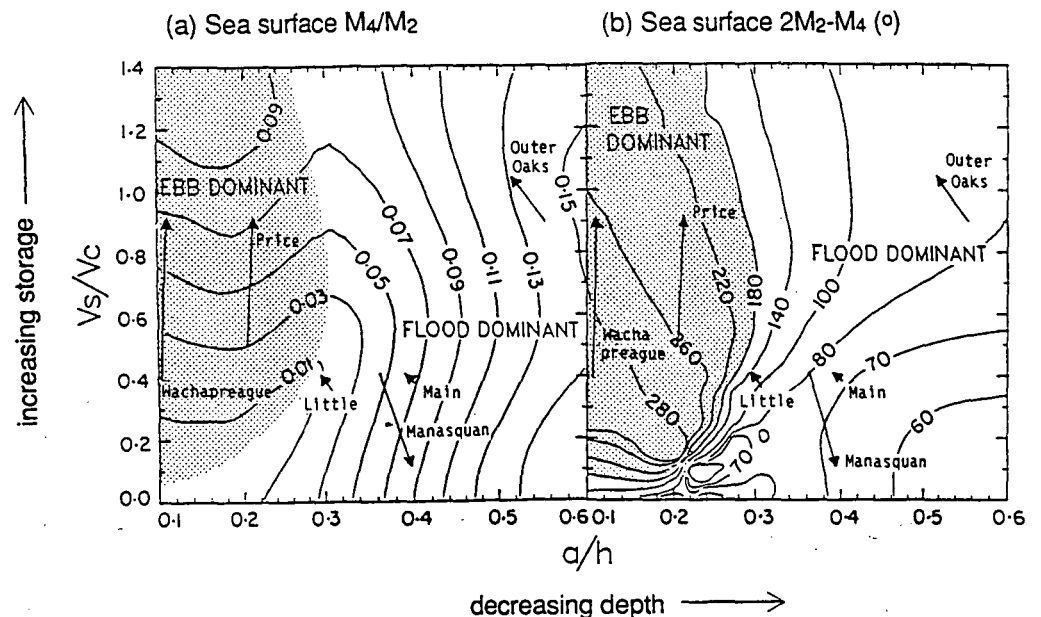

FIGURE 10. Changes in geometric parameters with sea-level rise at six tidally dominated estuaries, superimposed upon the results of numerical modeling: (a) surface M_4/M_2 amplitude ratio; (b) surface $2M_2-M_4$ relative phase. Arrows depict paths of a/h and Vs/Vc from relative mean sea level of -40cm to present mean water level. Paths indicate predicted changes in non-linear tidal distortion with sea level based upon hypsometry and numerical modeling.

IV. Distortion and Sea Level

Once changes in geometric parameters are determined as a function of sea level, initial trends in tidal distortion with global sea-level rise can be predicted. Paths illustrating variations in a/h and Vs/Vc with sea level are super-imposed upon contour plots of distortion versus geometry (Figure 10) to indicate predicted

changes in M_4/M_2 and $2M_2$-M_4. Main Creek and Little River are relatively shallow ($0.3 < a/h < 0.4$) having bank slopes of low curvature, whereas Price and Wachapreague are deeper ($0.1 < a/h < 0.2$) and have highly curved banks. Each pair of systems displays a common trend for the predicted path of non-linear distortion in response to changes in ocean height (Figure 10). Manasquan and Oaks Creek have different geometric features and correspondingly distinct predicted paths of non-linear response to relative sea level.

Table 2. Values for the parameters which describe system geometry, calculated for present sea level and for -40 cm.

	Relative sea level	a/h	Vs/Vc
Entire Main Creek, SC	Present	0.39	0.41
	-40 cm	0.40	0.39
Inner Main Creek, SC	Present	0.59	2.0
	-40 cm	0.67	1.7
Outer Main Creek, SC	Present	0.37	0.20
	-40 cm	0.36	0.24
Little River, SC	Present	0.29	0.41
	-40 cm	0.31	0.36
Price, SC	Present	0.21	0.92
	-40 cm	0.20	0.50
Wachapregue, VA	Present	0.11	0.91
	-40 cm	0.10	0.39
Manasquan, NJ	Present	0.40	0.11
	-40 cm	0.37	0.40
Entire Oaks Creek, SC	Present	0.55	1.5
	-40 cm	0.57	1.7
Inner Oaks Creek, SC	Present	0.62	3.2
	-40 cm	0.63	3.4
Outer Oaks Creek, SC	Present	0.52	1.05
	-40 cm	0.55	0.90

Harmonic analyses of tide gauge records are compared to variations in seasonal mean sea level to evaluate trends predicted by hypsometry and numerical modeling. Hourly sea heights are obtained from two sources: existing observational studies and the National Ocean Survey data banks. The method of least squares harmonic analysis is used to extract tidal components from the sea-surface data (Boon and Kiley, 1978). Data analysed at each station range in length from eight to fifteen months (~6,000-10,000 hrs), depending on available record. Analyses at each station are of subsamples of 697 hourly observations, spaced every 15 days (~1/2 subsample length) for sufficiently continuous sea height records. At each station linear regression is used to relate the parameters which quantify non-linear tidal distortion (M_4/M_2 and $2M_2$-M_4) to monthly mean sea level. The probability that the best-fit coefficient (β) has the same sign as the statistically "true" coefficient is determined using the t-test (Table 3). For this study, results of linear regression are defined as statistically significant for t-test coefficients greater than 0.9.

Trends in non-linear distortion produced by harmonic analyses of tide gauge data at Main Creek and Little River are consistent with predictions based upon hypsometry and numerical modeling. Geometric parameter paths (Figure 10) and results of linear regression (Table 3; Figure 11) suggest that for flood dominant systems with

relatively constant bank slope, M_4/M_2 decreases and $2M_2$-M_4 increases with an increase in relative sea level. For these systems, the decreased amplitude ratio along with increased relative phase indicate reduced flood dominance (and therefore reduced flood-to-ebb near-bed transport ratio). For flood dominant systems, magnitude of distortion (as measured by M_4/M_2) is primarily a function of a/h. Because the bank slopes of Main Creek and Little River are relatively constant, increased sea level causes mean channel depth to increase, a/h to decrease, and frictional effects on the tide to decrease. Thus observational and numerical results suggest that for flood dominant systems having relatively constant bank slope, the rate of channel shoaling is reduced with relative sea-level rise. If the initial values of a/h and Vs/Vc are near the 180° contour in $2M_2$-M_4, a large enough increase in mean sea level could conceivably alter the sense of tidal distortion from flood to ebb dominant, reversing the direction of net near-bed transport.

Table 3. Results of t-test relating monthly sea level to parameters describing non-linear tidal distortion. The equations are in the form $Y = \beta_0 + \beta_1 X$, where X = monthly sea level (with mean zero). [...] = probability that statistically 'true' coefficient is of same sign a β_1; N = number of observations.

	Y	β_0	β_1	N
Inner Main Creek, SC	M_4/M_2	0.094 [>.9999]	-0.076 [>.9999]	29
	$2M_2$-M_4(°)	90 [>.9999]	64 [>.9999]	
Outer Main Creek, SC	M_4/M_2	0.092 [>.9999]	-0.034 [.95]	23
	$2M_2$-M_4(°)	83 [>.9999]	-5 [.77]	
Little River, SC	M_4/M_2	0.054 [>.9999]	-0.079 [.9999]	12
	$2M_2$-M_4(°)	87 [>.9999]	-7 [.56]	
Price, SC	M_4/M_2	0.038 [>.9999]	0.031 [.995]	16
	$2M_2$-M_4(°)	244 [>.9999]	-16 [.99]	
Wachapregue, VA	M_4/M_2	0.042 [>.9999]	0.054 [>.9999]	22
	$2M_2$-M_4(°)	201 [>.9999]	20 [.82]	
Manasquan, NJ	M_4/M_2	0.092 [>.9999]	0.032 [.92]	26
	$2M_2$-M_4(°)	52 [>.9999]	20 [.93]	
Inner Oaks Creek, SC	M_4/M_2	0.082 [>.9999]	0.038 [.9992]	31
	$2M_2$-M_4(°)	112 [>.9999]	-72 [>.9999]	
Outer Oaks Creek, SC	M_4/M_2	0.074 [>.9999]	-0.104 [>.9999]	30
	$2M_2$-M_4(°)	77 [>.9999]	-24 [.97]	

Trends in non-linear distortion produced by harmonic analyses of tide gauge data at Price and Wachapreague are also consistent with predictions based upon hypsometry
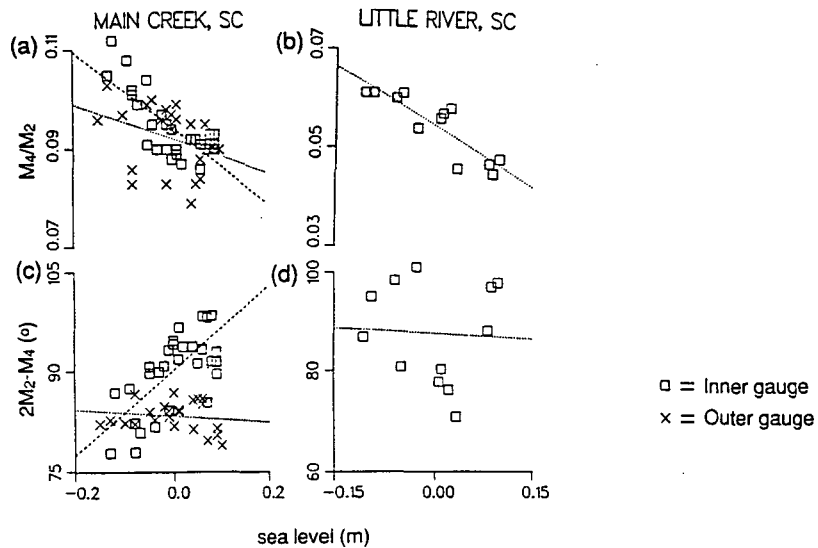
FIGURE 11. Parameters which determine non-linear tidal distortion at two flood dominant estuaries with relatively constant bank slope: surface M_4/M_2 amplitude ratio at (a) Main Creek, SC and (b) Little River, SC; surface $2M_2-M_4$ relative phase at (c) Main Creek and (d) Little River. Best-fit lines of linear regression are super-imposed upon results of a series of 697-hour harmonic analyses. Statistically significant regressions indicate that degree of flood dominance decreases with initial sea-level rise in this type of system.

and numerical modeling. Geometric parameter paths (Figure 10) and results of linear regression (Table 3; Figure 12) suggest that for ebb dominant systems having highly curved bank slopes, M_4/M_2 increases and $2M_2-M_4$ decreases with an increase in relative sea level. For ebb dominant systems, the increased amplitude ratio and decreased relative phase indicate increased ebb dominance (and therefore a greater ebb-to-flood near-bed transport ratio). For these systems, the magnitude of distortion is primarily a function of Vs/Vc. Because the bank slopes of Price and Wachapreague are highly curved, the volume of water stored intertidally and Vs/Vc increase dramatically with marginal increases in ocean height. Thus channel flushing is enhanced, the existing sense of tidal distortion is reinforced, and ebb dominant morphology may remain dynamically stable with higher mean sea level.

The trend in magnitude of non-linear distortion (M_4/M_2) produced by harmonic analyses of tide gauge data at Manasquan is consistent with the prediction of hypsometry and numerical modeling. The geometric parameter path (Figure 10) and results of linear regression (Table 3; Figure 13a) indicate that M_4/M_2 increases at Manasquan with an increase in relative sea level. However, predicted and observed trends for $2M_2-M_4$ relative phase are in disagreement, illustrating a limitation of this analysis technique. Manasquan is a shallow (mean channel depth 1.5m) lagoon with a dredged channel maintained along its axis (Figure 8a). Along much of the estuary the relatively deep dredged channel (low tide depth 2-3m) is bordered by broad shallows only 30-60cm deep at mean low water, which results in a highly curved bank slope. With seasonal sea-level rise at Manasquan, increasingly large sections of these shallows are submerged and become part of the momentum carrying central channel. For flood dominant systems, the magnitude of distortion (M_4/M_2) is primarily a function of a/h. Addition of the shallows to the main channel reduces average channel depth, increases a/h and increases the frictional effects on the tide. Thus landward near-bed transport is enhanced, the existing sense of tidal distortion is reinforced, and the need for dredging to maintain navigable channels may increase initially with higher mean sea level.
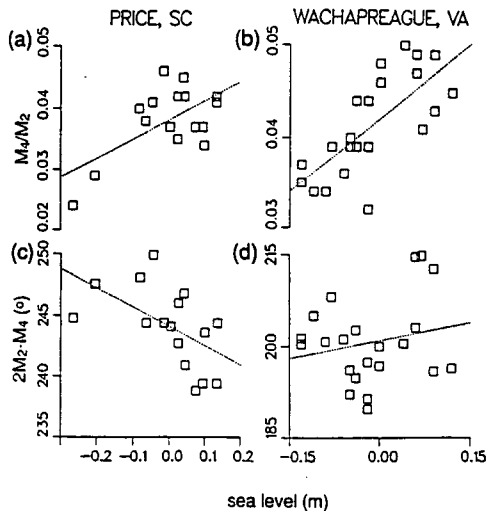
FIGURE 12. Parameters which determine non-linear tidal distortion at two ebb dominant estuaries with highly curved bank slope: surface M_4/M_2 amplitude ratio at (a) Price, SC and (b) Wachapregue, VA; surface $2M_2-M_4$ relative phase at (c) Price and (d) Wachapregue. Best-fit lines of linear regression are super-imposed upon results of a series of 697-hour harmonic analyses. Statistically significant regressions indicate that degree of ebb dominance increases with initial sea level rise in this type of system.
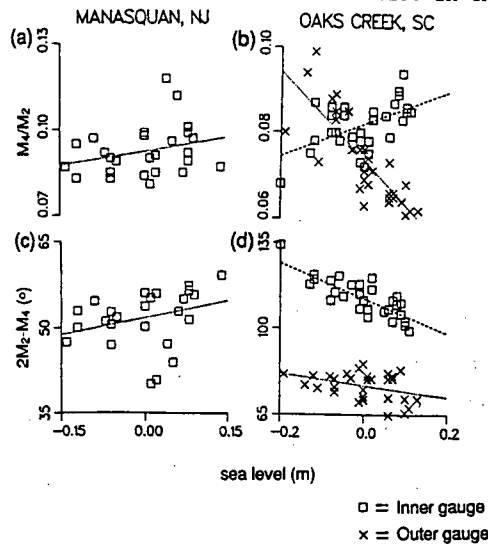

□ = Inner gauge
× = Outer gauge

FIGURE 13. Parameters which determine non-linear tidal distortion at two flood dominant estuaries with regions of highly curved bank slope: surface M_4/M_2 amplitude ratio at (a) Manasquan, NJ and (b) Oaks Creek, SC; surface $2M_2-M_4$ relative phase at (c) Manasquan and (d) Oaks Creek. Best-fit lines of linear regression are super-imposed upon results of a series of 697-hour harmonic analyses. The magnitude of tidal distortion (M_4/M_2) increases with sea level in regions of highly curved bank slope.

Changes in the magnitude of non-linear distortion in response to seasonal sea-level fluctuations is opposite at the two tide gauges at Oaks Creek (Figure 13b): At the inner gauge M_4/M_2 increases with sea-level rise whereas at the outer gauge M_4/M_2 decreases; $2M_2-M_4$ decreases with sea-level rise at both tide gauges. Oaks Creek is flood dominant, and for sea-level rise from -40cm to the present level a/h decreases (Table 2). Thus previous analysis techniques suggest M_4/M_2 should decrease and $2M_2$-M_4 should increase at both gauges. Aubrey and Friedrichs (1988) attributed the trends in non-linear distortion with sea level at the inner gauge to the proximity of locally extensive tidal flats. To test local geometric effects on changes in distortion with sea level rise, Oaks Creek is divided into inner and outer sections (Figure 8b). As a control, a similar division is made for the two gauges at Main Creek, which is also connected to the Atlantic Ocean via Murrells Inlet. Hypsometric curves for Main Creek and Oaks Creek (Figure 5a, f) are based on a bathymetric map of two foot (0.61m) contour interval, which includes the distribution and elevation of intertidal flats (Perry et al., 1978). This detail allows the determination of a/h values with a reasonable degree of confidence for a range of ocean heights, both below and above mean sea level (Figure 14). Because calculation of a/h is based upon depths of areas flooded at low water, it is not affected by uncertainties in marsh extent at high water.
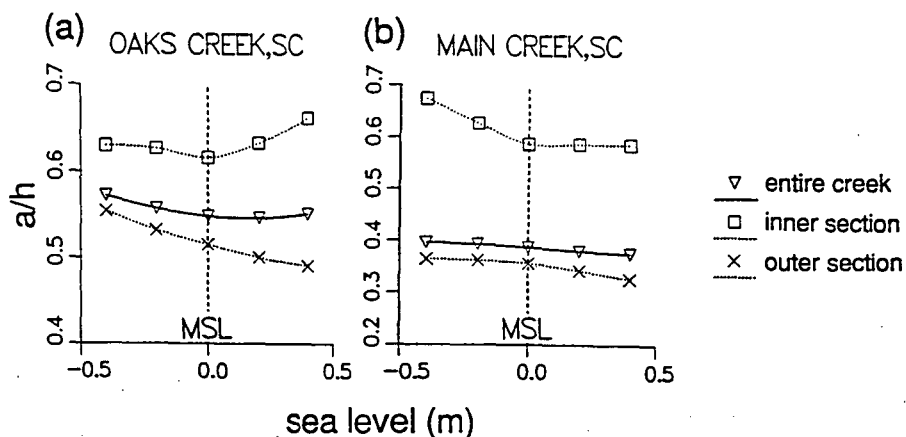

FIGURE 14. The a/h ratio as a function of relative sea level: (a) Oaks Creek, SC; (b) Main Creek, SC. Distinct trends in a/h with sea level in the inner and outer sections of Oaks Creek may account for opposite trends in local non-linear distortion with sea level in the two sections.

With sea-level rise, a/h is constant or continually decreasing for both sections of Main Creek and for the outer section of Oaks Creek (Figure 14). The a/h ratio increases with sea-level rise only for the inner section of Oaks Creek. The inner gauge at Oaks Creek also displays the only increase in M_4/M_2 with sea-level rise. Contrasts in bank slope in the two sections of Oaks Creek, as reflected in changes in a/h with sea-level rise, provide insight into the different trends in non-linear tidal distortion. Because bank slope in the outer section of Oaks Creek is relatively constant, increased sea level causes mean channel depth to increase and frictional effects on the tide to decrease. In contrast, locally extensive intertidal flats in the inner section of Oaks Creek contribute to a highly curved bank slope. A reduction in mean channel depth occurs as rising sea level incorporates former flats into the channel margins. Enhanced flood dominance in the inner section is reflected by the increase in M_4/M_2 and decrease in $2M_2$-M_4. The decrease in $2M_2$-M_4 at the outer gauge may reflect influences of the hypsometry of the inner section. In flood dominant systems having high bank curvature (such as

the inner section of Oaks Creek), higher mean sea level reinforces the existing sense of tidal distortion. In such systems flood dominant morphology may remain dynamically stable with higher mean sea level.

V. Discussion and Conclusions

Shallow tidally dominated estuaries will be among the environments to show clear effects of rising global mean sea level. In this study a methodology is developed to predict the initial impact of increased ocean height on tidal distortion in these systems. Measurements of the effects of seasonal mean sea-level fluctuations on estuarine tidal distortion combined with numerical modeling results are used to infer future near-bed sediment transport patterns and general trends in estuarine evolution.

Different estuarine responses to sea-level rise occur because non-linear tidal distortion is a composite of two principle effects: Frictional interaction between the tide and channels (reflected in a/h — offshore M_2 amplitude/mean channel depth) and intertidal storage in flats and marshes (measured by Vs/Vc — volume of intertidal storage/volume of channels at mean sea level). For strongly flood dominant systems distortion is primarily a function of a/h; for ebb dominant systems it is primarily a function of Vs/Vc.

Estuarine geometries, from which a/h and Vs/Vc are derived as functions of ocean height, are grouped into two categories: relatively constant and highly curved bank slope. In flood dominant systems having relatively constant bank slope, higher sea level causes mean channel depth to increase. The a/h ratio is decreased, and therefore the degree of flood dominance is reduced. If a/h is initially near the transition to ebb dominance, then a large enough increase in mean sea level can conceivably alter the sense of tidal distortion from flood to ebb dominant, reversing the direction of net near bed transport.

In ebb dominant systems having highly curved bank slope, marginally higher sea level substantially increases the volume of water stored intertidally. Vs/Vc increases, and therefore ebb dominance is enhanced. This reinforcement may result in ebb dominant morphology remaining dynamically stable as mean sea-level rises. The existing sense of distortion is also enhanced with rising sea level in flood dominant systems having highly curved bank slope. A reduction in mean channel depth occurs as higher water level incorporates former shallows and flats into the channel margins. The a/h ratio and the degree of flood dominance are increased. Thus for tidally dominated estuaries with banks of high curvature, sea-level rise can reinforce existing near-bed sediment transport patterns whether flood or ebb dominant. This may contribute to the stable evolution of passive margins during periods of transgression.

There are limitations to the application of this method to long range estuarine evolution. In discussing sedimentation patterns this analysis does not consider fine-grained suspended material, complex channel geometry, or episodic events such as storms. Furthermore, complicated non-linear processes are analysed through relatively simple physical and conceptual models. For instance, coupled interactions between hydrodynamics and hypsometry are ignored; given sufficient time, the hypsometry would respond to higher sea-levels, causing a change in hydrodynamics. The change in hypsometry is not included here. Nonetheless, significant relationships are demonstrated among estuarine geometry, sea-level rise, and trends in non-linear distortion. From these relationships trends for estuarine evolution in response to initial sea-level rise may be inferred. The method successfully predicts changes in non-linear tidal distortion due to small increases in sea level at a number of systems. Finally, the technique is not limited to the few geometries examined here, but can be extended to any tidally dominated estuary.

the Waterways Experiment Station's Coastal Engineering Research Center, and the Woods Hole Oceanographic Institution's Coastal Research Center.

VI. References

Aubrey, D. G., 1986: Hydrodynamic controls on sediment transport in well-mixed bays and estuaries. Physics of Shallow Estuaries and Bays, J. van de Kreeke, Ed., Springer-Verlag, New York, 245-258.

Aubrey, D. G., and C. T. Friedrichs, 1988: Seasonal climatology of tidal non-linearities in a shallow estuary. Hydrodynamics and Sediment Dynamics of Tidal Inlets, D. G. Aubrey and L. Weishar, Eds., Springer-Verlag, New York, 103-124.

Aubrey, D. G., and P. E. Speer, 1985: A study of non-linear tidal propagation in shallow inlet/estuarine systems. Part I: Observations. Estuarine, Coastal and Shelf Science, 21, 185-205.

Boon, J. D. III, 1988: Temporal variation of shallow-water tides in basin-inlet systems. Hydrodynamics and Sediment Dynamics of Tidal Inlets, D. G. Aubrey and L. Weishar, Eds., Springer-Verlag, New York, 125-136.

Boon, J. D. III, and R. J. Byrne, 1981: On basin hypsometry and the morphodynamic response of coastal inlet systems. Marine Geology, 40, 27-48.

Boon, J. D. III, and K. P. Kiley, 1978: Harmonic analysis and tidal prediction by the method of least squares. Spec. Report No. 186, Virginia Institute of Marine Science, Gloucester Pt., VA. 49 pp.

Byrne, R. J., P. Bullock and D. G. Tyler, 1975: Response Characteristics of a tidal inlet: a case study. Estuarine Research, Vol. 2: Geology and Engineering, L. E. Cronin, Ed., Academic Press, New York, 201-216.

Dronkers, J. J., 1964: Tidal Computations in Rivers and Coastal Waters, North Holland Publishing, Amsterdam. 516 pp.

Dronkers, J., 1986: Tidal asymmetry and estuarine morphology. Netherlands Journal of Sea Research, 20, 117-131.

Fitzgerald, D. M., and D. Nummedal, 1983: Response characteristics of an ebb-dominated tidal inlet channel. Journal of Sedimentary Petrology, 53, 833-845.

Friedrichs, C. T., and D. G. Aubrey, 1988: Non-linear tidal distortion in shallow well-mixed estuaries: a synthesis. Estuarine, Coastal and Shelf Science, 26, 521-545.

Giese, G. S., and D. G. Aubrey, 1987: Losing coastal upland to relative sea-level rise: 3 scenarios for Massachusetts. Oceanus, 30, 16-22.

Hoffman, J. S., D. Keyes and J. G. Titus, 1983: Projecting future sea level rise: methodology, estimates to the year 2100, and research needs. Report 230-09-007, U.S. Environmental Protection Agency, Washington, DC. 121 pp.

Jarrett, J. T., 1976: Tidal prism-inlet area relationships. G.I.T.I. Report 3, US Army Coastal Engr. Res. Cent., 55 pp.

Meyer-Peter, E., and R. Muller, 1948: Formulas for bedload transport. Proc. Second Meeting, International Association of Hydraulic Research, Stockholm, Sweden. pp. 39-64.

National Research Council (NRC), 1979: Carbon Dioxide and Climate: A Scientific Assessment, National Academy Press, Washington, DC. 496 pp.

National Research Council (NRC), 1987: Responding to Changes in Sea Level, National Academy Press, Washington, DC. 148 pp.

National Ocean Service (NOS), 1985: Index of Tide Stations: United States of America and Miscellaneous Other Locations. National Oceanic and Atmospheric Administration, Washington, DC. 143 pp.

Perry, F. C., W. C. Seabergh and E. F. Lane, 1978: Improvements for Murrells Inlet, South Carolina. Technical Report H-78-4, US Army Eng. Waterways Exp. Sta., Vicksburg, MI. 339 pp.

Postma, H. 1967: Sediment transport and sedimentation in the marine environment. Estuaries, G. H. Lauff, Ed., Amer. Assoc. Adv. Sci., Publ. 83, Washington, DC, 158-179.

Speer, P. E., and D.G. Aubrey, 1985: A study of non-linear propagation in shallow inlet/estuarine systems. Part II: theory. Estuarine, Coastal and Shelf Science, 21, 207-224.

Uncles, R. J. 1981: A note on tidal asymmetry in the Severn Estuary. Estuarine, Coastal and Shelf Science, 13, 419-432.